J Biomol NMR (2007) 39:337–342
DOI 10.1007/s10858-007-9198-y

NMR STRUCTURE NOTE

The NMR structure of the TRADD death domain, a key protein in the TNF signaling pathway

Désirée H. H. Tsao · Wah-Tung Hum · Sang Hsu · Karl Malakian · Lih-Ling Lin

Received: 9 August 2007 / Accepted: 18 September 2007 / Published online: 9 October 2007

Biological context

Tumor necrosis factor (TNF) is a member of a superfamily of cytokines that consists of more than 20 structurally related transmembrane and soluble proteins, which play a crucial role in various biological events by recruiting several intracellular adaptors, thus activating multiple signal transduction pathways (Wajant et al. 2003). TNF-α is a homotrimer produced by activated macrophages, and signals through two distinct cell surface receptor subgroups, TNFR1 and TNFR2. The cytoplasmic domain of these two receptors initiate intracellular events, with TNFR1 being the dominant receptor for TNF. The binding of TNF-α to TNFR1 triggers a series of intracellular events, involving many proteins which will recruit key enzymes to TNFR1 that are responsible for initiating signaling events, which leads to either apoptosis or activation of two transcription factors, NF-kB and AP-1. The cytoplasmic region of TNFR1 contains the death domain (DD) sequence, which forms a trimer upon formation of the TNF complex with TNFR1, recruiting other DD containing proteins such as TRADD (TNF receptor-associated DD), the adaptor protein RIP (receptor-interacting protein), and FADD (Fas-associated DD). These protein interactions occur mostly through their common domain, the DD, comprised of ~90 amino acids, with low (~30%) sequence homology. The DD superfamily is comprised of several subfamilies: DD, caspase recruitment domain (CARD), death effector domain (DED) and pyrin domain (PYR). So far, about 86 proteins have been identified in humans (Park et al. 2007).

The adaptor protein TRADD is a multifunctional 34 kDa protein that is recruited to TNFR1 upon ligand binding. It contains two separate domains, allowing it to bind to several protein partners and participate in different signaling pathways (Hsu et al. 1996). The C-terminal of TRADD contains a DD which is a central component in signaling for TNFR1 stimulation (Hsu et al. 1996). The DD of TRADD is recruited to TNFR1 through homotypic DD interactions, which then promotes subsequent binding to all other signal transducers. TRADD DD can associate to the death domains of TNFR1 and RIP (Hsu et al. 1996), while the N-terminal of TRADD interacts with TRAFs (TNF receptor associated factors), leading to NF-kB and MAP kinase activation.

The signaling events generated from TNFR1 upon ligand binding ultimately result in the inflammatory and immunological responses. These responses contribute to both physiological homeostasis and can lead to inflammatory diseases when TNF-α is overproduced. While the role of TNF-α in inflammatory diseases such as rheumatoid arthritis is clinically validated by several anti-TNF therapies, the question of how it triggers these specific signaling responses from TNFR1 by the complex array of signaling proteins remains to be fully understood. Many investigations have focused on understanding the mechanism by which these protein–protein interactions occur, including structural studies of proteins in the TNFR1 pathway. The three dimensional structure of the FAS DD (Huang et al. 1996), FADD DD (Carrington et al. 2006), TNF DD (Sukits et al.

D. H. H. Tsao (✉) · W.-T. Hum · K. Malakian
Structural Biology and Computational Chemistry, Chemical and Screening Sciences, Wyeth Research, 200 CambridgePark Drive, Cambridge, MA 02140, USA
e-mail: dtsao@wyeth.com

S. Hsu · L.-L. Lin
Inflammation Discovery Research, Wyeth Research, 200 CambridgePark Drive, Cambridge, MA 02140, USA

2001), among others, have been solved, and they all display a six-helix bundle structural fold, but with varied helix length and orientations. The surface features of the DD also vary, which could explain their different binding partners.

Here, we present the structure of human TRADD DD solved by NMR. The structure is composed of a six helix bundle similar to other DD, and its surface shows large positive and negative patches. The existing mutagenesis data (Park and Baichwal 1996; Sandu et al. 2005) is also compared with the current structure, in an effort to shed light into how these domains, and TRADD DD in particular, recognize their partners.

Methods and results

The DNA sequence containing residues 196–301 of TRADD and a C-terminal HIS tag was amplified by PCR and cloned in PRSETb. The sequence was confirmed by sequencing analysis. TRADD DD was expressed in BL21 *E. coli* cells with either $^{15}NH_4SO_4$ (2 g/l) or $^{15}NH_4SO_4$ and $^{13}C_6$glucose (2 g/l), and the protein was purified as described in Tsao et al. (2004).

All NMR spectra were collected on a 600 MHz Bruker Avance spectrometer at 25°C. The NMR data was processed with NMRPipe (Delaglio et al. 1995) and analysed with PIPP and STAPP (Garrett et al. 1991). For the backbone assignments, HNCACB and HN(CO)CACB experiments were performed. To confirm the type of amino acid assignment, C(CCO)NH-TOCSY (Grzesiek et al. 1993) was used. Side chain resonances were assigned from the following experiments: H(CCO)NH-TOCSY (Grzesiek et al. 1993) for the $^{15}N/^{13}C$ sample in 90% H_20, 10% D_2O, and HCCH-TOCSY for the $^{15}N/^{13}C$-labeled sample in D_2O, and ^{15}N- edited TOCSY-HSQC with the uniformly labeled ^{15}N protein. Stereospecific assignments for β-methylene protons and chi1 angles was obtained from the HNHB and ^{15}N-NOESY-HSQC with a mixing time of 40 ms. Stereospecific assignments of methyls in Leu residues were obtained from the 3D ^{13}C–^{13}C long range correlation (Bax et al. 1994), together with intra residue NOE intensity.

Distance restraints were obtained from ^{15}N-edited NOESY at 40 ms and 120 ms, and ^{13}C-edited NOESY at 94 ms experiments. Due to the high overlap of methyl resonances, the methyl–methyl NOE experiment with 100 ms mixing time (Zwahlen et al. 1998) was also performed for the identification of NOEs in the methyl region. Hydrogen bond restraints were obtained by analyzing a ^1H–^{15}N HSQC of TRADD DD by identifying slowly exchanging amide protons in a sample originally in H_2O exchanged into D_2O ($\sim$2 h exchange time). The HSQC showed signals from residues that are well protected. The restraints used are consistent with the observed NOESY crosspeaks as well as the values obtained for $^3J^{HN,H\alpha}$. Phi angle restraints were obtained by measuring the $^3J^{HN,H\alpha}$ coupling constant from the HNHA experiment (Vuister and Bax 1993). Residues with $^3J^{HN,H\alpha} < 6.5$ were constrained to $-60° \pm 30°$ in XPLOR calculations. Psi angles were obtained from TALOS predictions and only values with a score of 9 and 10 were used, for residues that have an experimentally determined Phi angle. Structures were calculated with a distance geometry/simulated annealing protocol of XPLOR 3.851, adapted to incorporate secondary $^{13}C\alpha/^{13}C\beta$ chemical shift and a conformational data base potential for the non-bonded contacts derived from high resolution x-ray structures (Kuszewski et al. 1996), with 1206 non redundant proton/proton distance restraints, 34 hydrogen bond distance restraints, 71 phi, 66 psi, 34 chi_1 and 8 chi_2 restraints. A summary of the statistics obtained is summarized in Table 1. The NOE distance restraints were categorized as strong (1.8–2.5 Å), medium (1.8–3.3 Å) and weak (1.8–5.0 Å).

Discussion and conclusion

The structure of TRADD-DD consists of a tightly packed arrangement of alpha helices in an anti-parallel fashion. Figure 1a displays the average minimized structure of TRADD-DD. The overlay of the 25 lowest energy structures is shown in Fig. 1b. The rmsd for the backbone atoms for residues 216–301 is 1.11 Å for all heavy atoms and 0.54 Å for structured regions. Table 1 summarizes the structural statistics for the ensemble of 25 structures. The N (residues 195–215) and C (residues 302–312) terminus are disordered, and there are six α-helices which form the canonical anti-parallel six helix bundle, characteristic of the DD superfamily. Helices 1 (L216-S225) and 4 (L261-E276) are on one side of the protein and helices 2 (K229-G240) and 5 (L282-E291) on the other side. Helix 3 (A248-R258) is located at the bottom of the helix bundle, while helix 6 (T295-L301) sits on top of the bundle. The helices are joined by short loops, and residues from all six helices contribute to the formation of the hydrophobic core.

To date, there are in total seven isolated DD structures solved (TNFR-1, FAS, FADD, P75 NGFR, IRAK4, RAIDD and Pelle. For references, see Park et al. 2007). The sequence identity between TRADD DD and the other DDs is low, varying between 16.9 (P75 NGFR) and 23.4% (TNFR-1). Despite this low identity, all DDs possess six helices. The size of the helices varies for each DD, but the overall arrangement of the six helix bundle is similar, with small variations on their relative positions. In fact, by superimposing the Cα atoms that compose the helical core,

Table 1 Structural statistics and rmsd for the 25 NMR derived structures for TRADD-DD

Structural statistics		
R. m. s. deviation from experimental distance restraints (Å)		
All (1206)	0.021 ± 0.001	
Intraresidual (369)	0.010 ± 0.002	
Sequential (341)	0.016 ± 0.001	
Short range (285)	0.022 ± 0.003	
Long range (211)	0.028 ± 0.003	
R.m.s. deviation from experimental torsional angle restraints (degrees)		
Φ (71), ψ $(66)^4$, $\chi_1 1$ (34), χ_2 (8)	0.33 ± 0.05	
R.m.s. deviations from experimental 13C shifts (ppm)		
13Cα (110)	1.03 ± 0.04	
13Cβ (110)	1.14 ± 0.03	
R.m.s. deviation from idealized covalent geometry		
Bonds (Å)	0.003 ± 0.0001	
Angles (°)	0.45 ± 0.007	
Impropers (°)	0.32 ± 0.001	
Ramachandran plot		
Most favorable region	94.3 ± 1.5	
Additionally allowed region	5.7 ± 0.8	
Generously allowed region	0	
Cartesian coordinate r.m.s. deviation (Å)		
	Secondary structure	Residues (216–303)
Backbone	0.51 ± 0.07	0.54 ± 0.07
Heavy atoms	1.07 ± 0.10	1.11 ± 0.10

The distance restraints were used with a square-well potential (Fnoe = 30 kcal mol^{-1} $Å^{-4}$). Medium-range NOEs are observed between protons separated by more than one and less than five residues in sequence. Long-range NOEs are observed between protons separated by five or more residues. No distance restraint was violated by more than 0.30 Å in any of the final structures. Hydrogen bonds were included as distance restraints and given the bounds of 1.8–2.3 Å (H–O) and 2.8–3.3 Å (N–O). The torsional restraints were applied with a force constant of 200 kcal mol^{-1} rad^{-2} (±30°) and no torsional restraint was violated by more than 5° in any of the structures. Psi angle restraints were obtained from TALOS (Delaglio 1997). Only values that had a score of 9 or 10 were used for residues that also had a Phi angle from the HNHA experiment. The carbon chemical shift restraints were applied with a force constant of 0.5 kcal mol^{-1} ppm^{-2}. A conformational database potential based on the populations of various combinations of torsion angles observed in a database of 70 high-resolution (1.75 A or better) X-ray structures was used, with a force constant of 1.0 (Kuszewski et al. 1996). The program PROCHECK was used to assess the quality of the structures. The precision of the atomic coordinates is defined as the average rms difference between the 25 final calculated structures and the mean coordinates. The backbone atoms comprise of N, Cα, C′ and O atoms

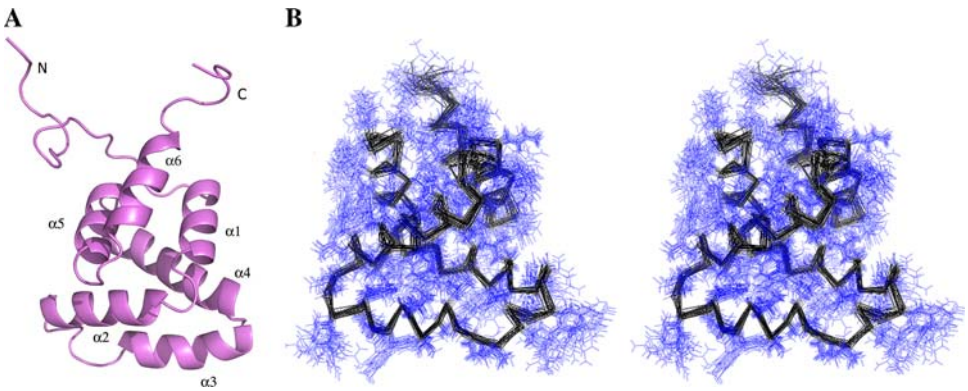

Fig. 1 Structure of TRADD DD. (**a**) Ribbon representation of the minimized average structure. (**b**) Stereo view showing the backbone and side chains of 25 superimposed structures (residues 214–304). The unstructured N and C termini are not shown

an rmsd range of 1.8–2.0 Å is observed between TRADD DD and TNFR1 DD, FAS DD and FADD DD.

Most of the hydrophobic residues are packing the core of the protein, except for L216, F254, the prolines at the N-terminal (P196, P197, P198) and L311 and A312 at the disordered C-terminal. Similar to the other death domains, there are several charged residues, and the biggest positively charged cluster is around helix 3. Figure 2a and b shows the patches on the surface on TRADD. A large positively charged patch is formed by seven arginines and lysines on one side of the protein (Fig. 2a), comprising of residues from helix 3, and the loop between helices 3 and 4 (K229, R231, R232, R235, R239, R242, R245). Three glutamic acid residues from helix 5 (E287, E290, E291) form a negative charged region adjacent to the positive patch. These charged patches on the surface of TRADD DD have been observed in other DD as well (Sukits et al. 2001; Huang et al. 1996; Carrington et al. 2006). Since the surfaces of many DD are highly charged, these patches have been proposed to be potential sites of interaction between the DDs.

In an effort to elucidate which parts of DD proteins are involved in self-association and protein/protein associations, many mutational studies have been performed on several proteins of this class, including TRADD DD (Park and Baichwal 1996; Sandu et al. 2005). An alanine scan was performed on TRADD DD (Park and Biachwal 1996), as an attempt to dissect the various binding activities of TRADD. Thirty-three mutants were generated, where 3–4 contiguous amino acids were mutated to Alanine along the TRADD DD sequence (aa 195–305). The authors find that the binding activity of TRADD DD (self association and binding to TNFR-1 DD) was reduced for residues mutated over the entire DD, leading to the conclusion that there were no specific regions on TRADD DD that were responsible for TRADD DD multimerization or binding to

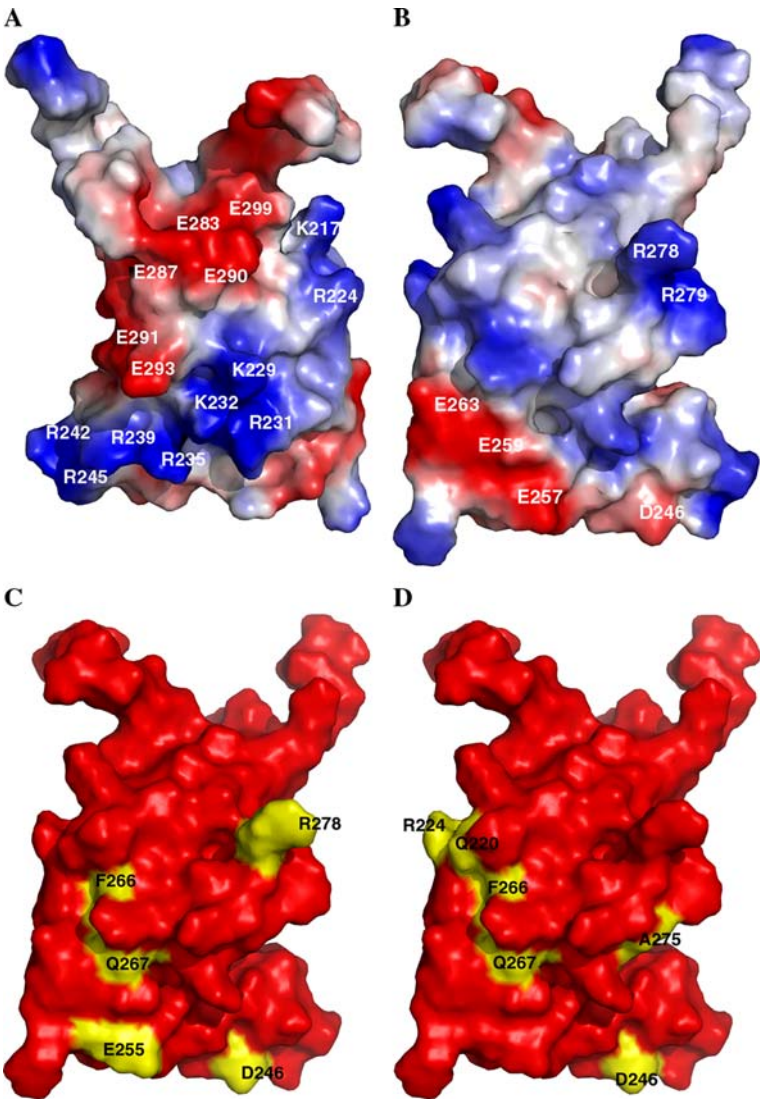

Fig. 2 Surface representation of TRADD DD. (**a**) Electrostatic surface potential with basic residues shown in blue and acidic residues in red. (**b**) Electrostatic surface as in (**a**), with a rotation by 180° along the X axis. (**c**) Residues of TRADD DD which were mutated in Sandu et al. 2005, highlighted in yellow on the surface (same orientation as (**a**)). These mutants failed to associate with FADD DD. (**d**) Residues of TRADD DD which were mutated in Sandu et al. 2005, highlighted in yellow on the surface (same orientation as panel (**b**)). These mutants failed to associate with TNFR-1 DD. All figures and electrostatic calculations were made using the program PyMOL (http://www.pymol.org)

TNFR-1, but rather, the whole protein was important for function. In addition, the mutants were also evaluated for their ability to activate NF-kB, and many mutants did not activate NF-Kb. Similar to the mutant binding activity results, there was no correlation between NF-Kb activation and the location of the mutations along TRADD DD sequence.

This mutational analysis performed on TRADD DD was very comprehensive and encompassed the full sequence of the DD. It was concluded from this study that the TRADD DD functions as a whole for the different activities, and no discrete region of the protein was responsible for any particular function. Care must be taken in interpreting the mutation results, as many mutant proteins could have lost activity because the structure of the protein may no longer be intact. Mutations that were found to retain the most activity are located at either the N or C termini of the protein or in non-structured regions. Many residues that were mutated along TRADD DD sequence were residues that form the hydrophobic core of the protein, and this would likely result in disruption of the structural integrity of the protein, thus leading to the lack of activity. Residues such as V226, L228, W230, V233, L237 are among many that were mutated and are crucial in maintaining the protein fold.

More recently, selective mutation studies on DD, which includes TNFR1, FADD and TRADD, along with pull-down binding assays, have suggested that TRADD DD uses the same surface to interact with the DD of FADD and TNFR1 (Sandu et al. 2005). Out of the 28 TRADD DD mutants made, five (D246R, E255R, F266E, Q267A, R278A) completely lost binding activity towards full length FADD. They fall on one side of TRADD DD (Fig. 2c), suggesting that this surface is responsible for binding to FADD. Based on our structural work, residues F266 and Q267 are involved in a small network of interactions with other residues in the protein, suggesting they are crucial for the structural integrity of TRADD DD. Mutation of these residues would likely impact the overall folding of the protein. D246R, E255R and R278A mutations have a much lower impact on the overall protein structure, as these side chains are completely exposed and thus accessible for interactions with FADD DD.

Six TRADD DD mutants affected binding to TNFR1 DD, including the same residues that affected interactions with FADD, D246R, F266E and Q267A. The structure of TRADD DD shows that possibly only D246R could be important for binding, as this residue is completely exposed, thus available to form interactions. Three other TRADD DD mutants which also disrupted the interaction with TNFR1 DD are Q220E, R224E and A275A (Fig. 2d). The side chain of R224 extends outwards on the surface (Fig. 2a, d), near the large positive charged patch. Interestingly, mutations of charged residues located on this surface of TRADD DD (Fig. 2a) had no or minimal effect on the binding to TNFR1 and FADD, as observed for six mutations located in helices 2 and 6 (R231A, R235A, E290R, E291A, N292D, E293R and E299A). This suggests that the majority of positive and negative surfaces on TRADD may not play an important role in protein association. It is possible that these sites may be involved in the interaction with a yet unidentified protein. Progress continues to be made towards unraveling the different modes of interactions between the death domains, but additional biochemical and structural studies are needed to elucidate what drives these domains to engage in these protein/protein interactions as well as understanding the molecular basis of these interactions.

References

Bax A, Delaglio F, Grzesiek S, Vuister GW (1994) Resonance assignment of methionine methyl groups and $\chi 3$ angular information form long-range proton-carbon and carbon–carbon J correlation in a calmodulin-peptide complex. J Biomol NMR 4:787–797

Carrington PE, Sandu C, Wei Y, Hill JM, Morisawa G, Huang T, Gavathiotis E, Wei Y, Werner MH (2006) The structure of FADD and its mode of interaction with procaspase-8. Mol Cell 22:599–610

Delaglio F, Grzesiek S, Vuister GW, Zhu G, Pfeifer J, Bax A (1995) NMRPipe: a multidimensional spectral processing system based on UNIX pipes. J Biomol NMR 6:277–293

Garrett DS, Powers R, Gronenborn AM, Clore GM (1991) A common sense approach to peak picking two-, three- and four-dimensional spectra using automatic computer analysis of contour diagrams. J Magn Reson 95:214–220

Grzesiek S, Anglister J, Bax A (1993) Correlation of backbone amide and aliphatic side-chain resonances in $^{13}C/^{15}N$-enriched proteins by isotropic mixing of ^{13}C magnetization. J Magn Reson B 101:114–119

Hsu H, Shu HB, Pan MG, Goeddel DV (1996) TRADD-TRAF2 and TRADD-FADD interactions define two distinct TNF receptor 1 signal transduction pathways. Cell 84:299–308

Huang B, Eberstadt M, Olejniczak ET, Meadows RP, Fesik SW (1996) NMR structure and mutagenesis of the Fas (APO-1/CD95) death domain. Nature 384:638–641

Kuszewski J, Gronenborn AM, Clore GM (1996) Improving the quality of NMR and crystallographic protein structures by means of a conformational database potential derived from structure databases. Protein Sci 5:1067–1080

Park A, Baichwal VR (1996) Systematic mutational analysis of the death domain of the tumor necrosis factor receptor 1-associated protein TRADD. J Biol Chem 271:9858–9862

Park HH, Lo YC, Lin SC, Wang L, Yang JK, Wu H (2007) The death domain superfamily in intracellular signaling of apoptosis and inflammation. Annu Rev Immunol 25:561–586

Sandu C, Gavathiotis E, Huang T, Wegorzewska I, Werner MH (2005) A mechanism for death receptor discrimination by death adaptors. J Biol Chem 280:31974–31980

Sukits SF, Lin LL, Hsu S, Malakian K, Powers R, Xu GY (2001) Solution structure of the tumor necrosis factor receptor-1 death domain. J Mol Biol 310:895–906

Tsao DH, Hum WT, Hsu S, McGuire M, Malakian K, Lin LL (2004) Assignment of ^{1}H, ^{13}C and ^{15}N resonances of the death domain of TRADD. J Biomol NMR 4:407–408

Vuister G, Bax A (1993) Quantitative J correlation: a new approach for measuring homonuclear three-bond $J(H^{N}H^{a})$ coupling constants in ^{15}N-enriched proteins. J Am Chem Soc 115:7772–7777

Wajant H, Pfizenmaier K, Scheurich P (2003) Tumor necrosis factor signaling. Cell death and differentiation 10:45–65

Zwahlen C, Gardner KH, Sarma SP, Horita DA, Byrd RA, Kay LE (1998) An NMR experiment for measuring methyl–methyl NOEs in ^{13}C-labeled proteins with high resolution. J Am Chem Soc 120:7617–7625